Strathprints Institutional Repository

Mandal, Paranjayee and Paul, Soumitra (2012) Effect of alloyed target vis-à-vis pure target on machining performance of TiAlN coating. International Journal of Advanced Manufacturing Technology, 66. pp. 721-731. ISSN 0268-3768 , http://dx.doi.org/10.1007/s00170-012-4360-4

Int J Adv Manuf Technol
DOI 10.1007/s00170-012-4360-4

ORIGINAL ARTICLE

Effect of alloyed target vis-à-vis pure target on machining performance of TiAlN coating

Q1 **Paranjayee Mandal · S. Paul**

Received: 13 August 2011 / Accepted: 26 June 2012

Abstract Typically closed-field unbalanced magnetron sputtering (CFUBMS) and controlled cathodic arc deposition techniques having four or six pure or alloyed targets are employed for commercial titanium aluminium nitride (TiAlN) coating of cutting tools. The role of the use of alloyed target vis-à-vis pure target on the coating characteristics and the machining performance of TiAlN-coated tools has not been studied in detail. In the present work, TiAlN coating has been deposited on cutting tools using a pulsed DC, dual-cathode CFUBMS system to capture the role of the type of target on machining performance. The deposition rate in the case of the alloyed target has been found to be much higher as compared to the pure target. Such coatings deposited from alloyed targets also provided significantly better machining performance in dry turning of low-carbon and high-carbon steel. Dry turning of SAE 1070 high-carbon steel at 160 m/min did not yield more than 100 μm of average flank wear on the same insert coated using alloyed targets for a machining time of more than 3 min.

Keywords TiAlN coating · Pulsed DC closed-field unbalanced magnetron sputtering · Pure target · Alloyed target · Machining performance

1 Introduction

Physical vapour deposition (PVD)-coated cutting tools are very efficient in enhancing productivity in the metal cutting industry. They are preferred over chemical vapour deposition (CVD)-coated cutting tools owing to the lower deposition temperature (300–500 °C). The most common are the titanium nitride (TiN)-coated tools, which are widely used as protective hard coating to increase the lifetime and performance of cutting and forming tools. Munz [1] reported that the main drawback of TiN-coated tools is that they are easily oxidized at 550 °C and form poor adherent and a brittle titanium dioxide (TiO_2) layer on top of the TiN layer. Because of the large difference in the molar volume of TiO_2 and TiN, compressive stresses are developed in the oxide layers and spallation takes place. Therefore, the protecting ability of the TiN coating is lost. To overcome such a problem and to improve the mechanical properties of TiN coating, the incorporation of a third element, like Al, Si, Cr, or Zr, to the TiN film has been suggested to form a ternary composite coating so that the new multicomponent films can yield superior oxidation resistance and increase the tool life significantly compared to conventional TiN coating. Lee et al. [2] have studied the effect of the incorporation of Cr on the structure and properties of titanium chromium nitride ((TiCr)N) coating and inferred that an increase in Cr content led to a beneficial effect on wear resistance and coating hardness. Santana et al. [3] have reported that the addition of Al enhances the thermal stability of TiAlN coating.

Since the mid 1980s, TiAlN coating had been successfully developed as a promising alternative to TiN-coated cutting and forming tools. Munz [1] developed TiAlN coating using sputter ion-plating process and reported the performance of TiAlN-coated drills to be two times better than that of TiN-coated ones. In recent years, TiAlN coating has been given much attention because of its high anti-oxidation property (it is oxidized at 800 °C), high hardness, high corrosion resistance and lower thermal conductivity, as reported by Munz [1]. McIntyre et al. [4] experimentally investigated the kinetics and mechanism of the oxidation of

P. Mandal (✉) · S. Paul
Department of Mechanical Engineering,
Indian Institute of Technology Kharagpur,
Kharagpur 721 302, West Bengal, India
e-mail: 200712mum@gmail.com

S. Paul
e-mail: spaul.mech@iitkgp.ernet.in

TiAlN films and observed that when the TiAlN film is exposed to high temperatures, it reacts with oxygen and forms a dense, highly adhesive aluminium oxide (Al_2O_3) layer on top of the coating, protecting it from further oxidation. Thus, TiAlN film exhibits good anti-oxidation behaviour that helps in reducing adhesive wear, which is the major wear mechanism in the cutting tool. Another major advantage of the TiAlN coating is its lower thermal conductivity, as cited by Hsieh et al. [5], which helps in the dissipation of more heat via chip. Therefore, thermal loading on the substrate reduces permitting higher cutting speeds.

Closed-field unbalanced magnetron sputtering (CFUBMS) using pure DC and pulsed DC, and controlled cathodic arc deposition of TiAlN have been well-researched areas. Kelly et al. [6] commented that the advent of pulsed DC CFUBMS could successfully address the issues of low deposition rate and target poisoning effectively whilst experimentally investigating the reactive unbalanced magnetron sputtering of aluminium oxide coating. Most researchers have used four or six target machines using DC or the pulsed DC CFUBMS technique for the deposition of TiAlN. They have used both pure as well as alloyed targets. However, a survey of previous literature could not yield much information on TiAlN coating developed using dual-cathode deposition systems employing pulsed DC, reactive closed-field unbalanced magnetron sputtering with pure and alloyed targets.

A survey of previous technical papers in the public domain indicates the availability of little systematic information regarding the machining performance of TiAlN-coated tools whilst turning carbon steels. Jindal et al. [7] used PVD-coated TiN, titanium carbo-nitride (TiCN) and TiAlN-coated cemented carbide tools and compared their machining performance whilst turning SAE 1045 medium-carbon steel at cutting velocities of 305 and 396 m/min, feed of 0.15 mm/rev and depth of cut of 0.75 mm under a wet machining environment. The tool life criteria used have been average flank wear, VB, of 0.4 mm or maximum flank wear, VB_{max}, of 0.75 mm. They found the average flank wear to be only 0.2 mm after 60 min of machining when the cutting velocity was 305 m/min, but the tool life was only 25 min when the cutting velocity was raised to 396 m/min for TiAlN-coated carbide inserts. Khrais and Lin [8] used commercial PVD-applied TiAlN-coated cemented carbide inserts (6 % cobalt) for turning AISI 4140 steel at a cutting velocity of 210–410 m/min, feed of 0.14 mm/rev and depth of cut of 1 mm under both wet and dry cutting conditions. They reported that with the increase in cutting speed from 210 to 410 m/min, tool life decreased from 65 to 5 min. TiAlN-coated tools performed best under dry cutting for a cutting speed of <260 m/min.

Moreover, information regarding the comparison of the machining performance of TiAlN-coated inserts deposited from pure targets as well as alloyed targets has not been found. Thus, the objective of the present study was to investigate the role of alloyed targets vis-à-vis pure targets on the characteristics and machining performance of TiAlN coating deposited in a dual-cathode pulsed DC CFUBMS system whilst turning different carbon steels.

2 Experimental details

TiAlN coating was deposited in a dual-cathode pulsed DC, closed-field unbalanced magnetron system (VTC-01A) manufactured by Milman Thin Film Systems Pvt. Ltd., India. The coating system is shown photographically in Fig. 1. Coating had been deposited on three different types of substrates, namely, HSS block of M2 grade (10×10×20 mm), low-carbon steel (SAE 1010) disc-shaped coupons (ϕ=25×10 mm) and uncoated tungsten carbide inserts of grade K10 (94 % WC+6 % Co) and nominal geometry SNMA 120408. Prior to deposition, all substrates except the inserts were polished to a roughness of R_a=0.05 μm and ultrasonically cleaned using acetone, trichloroethylene, isopropyl alcohol and distilled water. Before transferring the samples to the deposition chambers, they were dried using hot air. For three samples (S7, S8 and S9), one pure titanium and one pure aluminium target were used, whereas for two samples (S10 and S11) alloyed titanium–aluminium targets (atomic ratio Ti/Al=60:40) were used. All the targets had purity better than 99.99 %, with a dimension of 254×127 mm and a thickness of 12 mm. The substrate stage had a twofold rotation facility and was imparted a rotational speed of 4 rpm during deposition. Bipolar pulsed DC power supplies (Advanced Energy Pinnacle Plus) were used. Cathodes were energized in current mode and the substrate

Fig. 1 Photograph of the coating system

energized in voltage mode. A base pressure of better than 2×10^{-3} Pa was achieved prior to initiating deposition, which is very similar to the base pressure reported by Musil and Hruby [9] and Zhou et al. [10].

The deposition cycle consisted of sputter cleaning of the targets with shutters in closed position, followed by ion etching. Ion etching was conducted at a bias voltage of −500 V with a pulsed frequency of 250 kHz at Ar pressure of 0.16 Pa, with the titanium target current set to 1 A. Then, a titanium interlayer of around 200-nm thickness (for S7, S8 and S9) or a titanium–aluminium interlayer (for S10 and S11) was deposited. This was followed by a TiN interlayer for samples S7, S8 and S9. Other relevant deposition parameters are given in Table 1.

The surface morphology and the fractograph of the coated samples were observed under a scanning electron microscope (Carl Zeiss EVO 60) fitted with an energy-dispersive X-ray (EDX) analyser (INCA FET 3X). The composite Vicker's micro-hardness of the coating was measured using a load of 1 N with a dwell time of 15 s in a LECO LM-700 micro-hardness measurement system. For each sample, ten measurements were taken; their average has been reported.

The adhesion of the coating to the substrate has been measured by a TR-101 M5 DUCOM Scratch Tester with five replicates. Testing was undertaken with a Rockwell C diamond indenter having a tip radius of 0.2 mm. The indenter was drawn across the coating at a speed of 6 mm/min over a scratch length of 15 mm. The normal load during scratching was varied from 10 to 120 N.

The scratch adhesion is quantified by the normal load at which the coating fails. This is typically termed as the critical load or L_C. In the present work, the critical load has been determined by the sudden increase in the ratio of the tangential or traction force to the normal force during scratching. This typically coincides with the L_{C3} type of failure which indicates initiation of removal of the coating from the scratch, as has been reported by He et al. [11]. All the above tests were performed on coated HSS M2 samples.

Table 1 Deposition parameters for as-deposited TiAlN coating

Ar flow rate	15 sccm
N_2 flow rate	10 sccm
Chamber pressure of Ar	0.20 Pa
Partial pressure of N2	0.07 Pa
Ti target current (for pure target)	3 A
Al target current (for pure target)	4 A
Ti:Al target current (for alloyed target)	5 A
Substrate bias voltage	−50 V
Deposition temperature	300 °C (S8, S9)
	350 °C (S7, S10, S11)
Target frequency	200 kHz (S8, S10)
	250 kHz (S7)
	300 kHz (S9, S11)
Duty cycle	80 %

Ball-on-disc tests were performed using a tribometer (TR-201 M3 DUCOM) to study the tribological performance of the coating. The tests were undertaken at a normal load of 10 N using 5-mm diameter cemented carbide balls (WC=94 % and Co=6 %) with a sliding speed of 200 mm/s under ambient conditions (25 °C and 50 % relative humidity). The depth of the wear track was measured at five different locations using contact-type surface profilometer (Taylor-Hobson Surtronic 3+).

The machining performance of the coated tungsten carbide inserts was evaluated by dry turning of as-rolled and proof-machined, low-carbon steel (SAE 1020 with 143 BHN) and annealed and proof-machined, high-carbon steel (SAE 1070 with 198 BHN) bars. The choice of high-carbon steel for the evaluation of cutting performance is common as high-carbon steels are difficult to machine. On the other hand, the problem with low-carbon steel is its ductility and toughness. Many of the previous researchers [12–15] had also used low-carbon steels for estimating the machining performance of coated (PVD/CVD) cutting tools. Hence, these two types of work materials have been chosen to evaluate the machining performance of TiAlN-coated inserts in the present study. Table 2 lists all the machining parameters. Machining was interrupted at regular intervals, and the rake and flank faces of the cutting tool were inspected under a stereo zoom microscope (Olympus model SZ 1145TR PT zoom stereomicroscope) fitted with a digital photomicrograph system (Olympus C-5060 wide zoom). The cutting tools were ultrasonically cleaned in acidic solution before such inspection to remove any work material built-up on the rake face. The average and the maximum flank wears were determined from the photomicrographs.

Normally, P-grade uncoated carbide inserts are used to machine steels because they are diffusion-resistant due to the presence of titanium carbide (TiC), tantalum carbide (TaC) and niobium carbide (NbC). K-grade uncoated inserts (plain WC inserts without any alloying carbides) are used in machining grey cast iron and nonferrous metals. The deposition of coating leads to a reduction in toughness or transverse rupture strength, particularly for CVD coating [16]. Therefore, to obtain an adequate balance between toughness and hardness of the cutting tool insert, tough and wear-resistant K-grade inserts are generally coated [7,16,17].

3 Results and discussion

Figure 2 shows the surface morphology and the fractograph of representative coatings, namely, S8, S10 and S11. The SEM photographs depicting the surface morphology have been acquired at ×10,000, whereas the SEM photographs revealing the fractographs are at ×3,000. This strategy has

Table 2 Detailed machining parameters for dry turning

Work material	SAE 1020 and SAE 1070 steel	
Chemical composition of work material as provided by optical emission spectroscopy	SAE 1020 steel	SAE 1070 steel
	0.19 % C, 0.074 % Si, 0.374 % Mn, 0.043 % P, 0.03 %S, 0.02 % Cr, rest Fe	0.716 % C, 0.223 % Si, 0.74 % Mn, 0.018 % P, 0.022 %S, 0.003 % Cr, rest Fe
Inserts used	TiAlN-coated carbide (coated in-house)	
Substrate grade	K10	
Insert designation	SNMA 12 04 08	
Tool holder specification	PSBNR 2525M12	
Q4 Tool geometry	−6°, −6°, 6°, 6°, 15°, 75°, 0.8 (mm)—orthogonal rake system	
Cutting velocity (m/min)	250 (for SAE 1020 steel)	
	160 (for SAE 1070 steel)	
Feed (mm/rev)	0.2	
Depth of cut (mm)	2	
Environment	Dry	

been adopted to clearly reveal interesting features on the surface and on the fractograph. The coating morphology of the S8 sample deposited from pure target looks finer; hence, an inset SEM photograph (Fig. 2g) has been added at ×30,000 to clearly reveal the morphology. Similarly, the coating thickness on sample S8 is much smaller as compared to the coating thickness obtained on samples S10 and S11. Thus, an inset SEM photograph (Fig. 2h) has been added for sample S8 at ×30,000. For sample S8, which has been deposited from pure targets, the agglomerated grain size seems to be sub-micronic, as can be seen in Fig. 2g. The coating also looks very compact both in the top view (Fig. 2g) and the fractograph (Fig. 2h). Similar compact nanocrystalline coatings have been reported by Bhaduri et al. [19] for TiN deposited using dual-cathode reactive CFUBMS. The fractograph (Fig. 2h) reveals a dense columnar structure, though it may not be termed as featureless, which was once again reportedly obtained for TiN coating at high negative bias voltage by Bhaduri et al. [19]. On the other hand, the samples (S10 and S11) obtained using alloyed targets provided much thicker coatings for the same coating cycle duration. But the coating consisted of large overgrowths, as can be seen in Fig. 2b, c. The fractographs (Fig. 2e, f) also reveal a clear columnar structure which did not resemble dense coating. The higher coating thickness for alloyed targets may be attributed to the higher target current density. Furthermore, in the case of pure targets, the dual-cathode configuration (Q5) seems to be not very effective for a high deposition rate as Ti and Al targets were sputtered from opposite directions. Most of the previous literature indicates the use of four or six target machines.

Table 3 shows the chemical composition of the as-deposited coatings obtained through bulk EDX analysis. For pure targets (samples S7, S8 and S9), $\left(\frac{\mathrm{Al}}{\mathrm{Ti+Al}}\right) \times 100$ ratio seems to be slightly more than 55, indicating this to be an Al-rich coating. This may be attributed to the higher target current density used for aluminium (4 A as opposed to 3 A for Ti targets). Oliveira et al. [20] reported the $\left(\frac{\mathrm{Al}}{\mathrm{Ti+Al}}\right) \times 100$ ratio to be 34.5 % for an aluminium target current of 1.75 A against a total operating current of 10.5 A, and an increase in the aluminium target current led to an increase in this ratio. While using alloyed targets, the same ratio was found to be around 36 in the present work, which almost indicates a transfer of the alloying percentage of the target to the coating despite reactive sputtering.

Table 4 summarizes the important coating characteristics. For a 9-h-long coating cycle, around 2 μm coating could be obtained from pure targets, providing a deposition rate of only 3.7 nm/min, whereas a coating thickness in excess of 12 μm could be obtained using alloyed targets. Thus, the deposition rate is around 22 nm/min when alloyed targets are used. Astrand et al. [21] reported a similar deposition rate (23 nm/min) for TiAlN coating using four pure targets in a pulsed DC CFUBMS system. Q7

The composite Vicker's micro-hardness for TiAlN coating has been measured to be just better than 21 GPa for pure targets. The literature indicates similar composite micro-hardness to be as much as 30–40 GPa. For example, Oliveira et al. [22] reported a depth-sensing indentation hardness of 36 GPa for TiAlN film at a measurement load of only 20 mN. Mushil and Hruby [9] similarly obtained a micro-hardness of better than 40 GPa with a indentation load of 15 mN. A nano-hardness of around 31 GPa was reported separately by Shum et al. [23] and Zywitzki et al. [24]. This may be attributed to a significant substrate effect as 1 N load was used for indentation in the present investigation. Any reduction in load led to a very small indentation, which prompted the choice of 1 N as the indentation load. The use of alloyed target provided composite micro-hardness values of around 21 GPa (S10) and 34 GPa (S11).

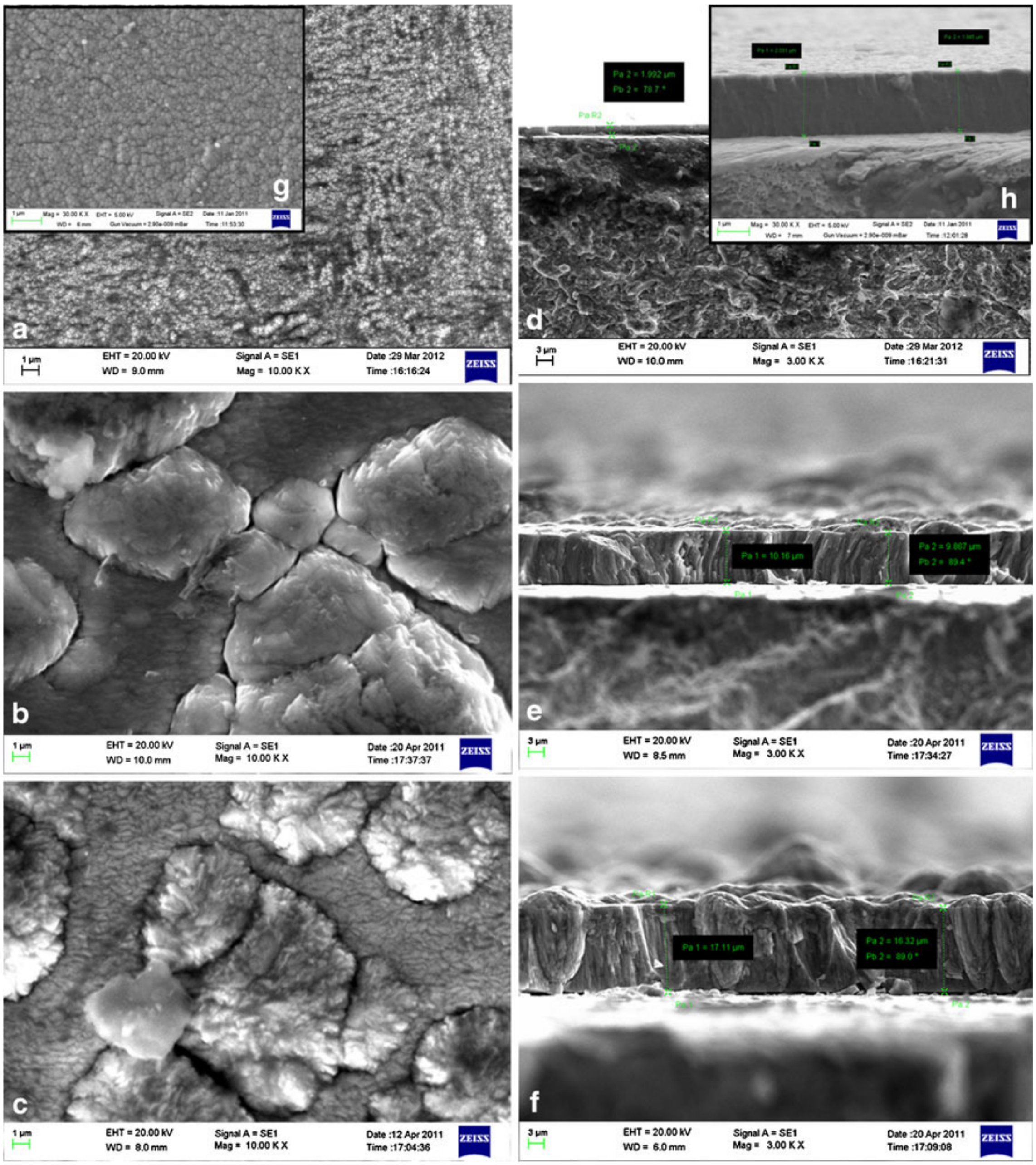

Q6 **Fig. 2** Surface morphology and fractograph of coatings—S8, S10 and S11

Table 3 Chemical composition of the as-deposited TiAlN coatings

Sample no.	Atomic percentage of elements				$\left(\frac{Al}{Ti+Al}\right)$
	Ti	Al	N	Fe	
S7	22.08	28.50	48.63	0.79	56.35
S8	22.14	29.02	48.2	0.63	56.72
S9	21.39	27.92	50.12	0.57	56.62
S10	36.59	23.08	40.33	0.0	36.68
S11	38.57	20.93	40.50	0.0	35.18

This clearly indicates the beneficial effect of a higher deposition frequency on the hardness of the coating as the same Q8 was 300 kHz for S11 compared to 200 kHz for S10. As the coatings are rather thick for samples S10 and S11, these two hardness values can be viewed as the coating hardness as the effect of the substrate is expected to be not very significant.

A hard wear-resistant coating also needs to have sufficient adhesion with the substrate for any useful application as a cutting tool. The effect of the type of target on the adhesion of the coating could not be captured in the present study, but a minimum critical load of around 51 N and a

Table 4 Coating properties of the as-deposited TiAlN coatings

Sample no.	Mechanical properties of coating			
	Coating thickness (μm)	Composite micro-hardness (GPa)	Critical load (N)	Wear coefficient ($\times10^{-15}$ m^3/Nm)
S7	2.18±0.01	22.54±4.19	60±15	5.63±0.97
S8	1.87±0.23	22.11±4.88	77.5±12.5	8.69±1.19
S9	2.06±0.06	21.69±5.39	70±15	9.52±1.19
S10	10.1±0.25	21.71±2.8	51.1±7	26.1±6.4
S11	12.5±5.00	34.7±6.29	86±4	27.2±6.4

maximum critical load of around 86 N were obtained for the whole experimental domain, as detailed in Table 4. TiN coatings deposited using a similar route provided lower critical load [19], whereas TiN–MoS_x coating yielded critical load in the range of 50–60 N [25]. Shum et al. [23] also reported around 70 N critical load for TiAlN coatings deposited using pure targets in a four-target machine.

The tribological performance of the coating has been accessed by the wear coefficient. The wear coefficient has been determined as the ratio of the total volume of the wear track to the product of normal load and sliding distance. A lower wear coefficient indicates better wear resistance of the coating in a ball-on-disc configuration. This configuration primarily simulates adheso-diffusive wear. However, the ball-on-disc test may also lead to a scenario of three-body abrasion if the hard coating fragments during the test; a similar situation has been reported by Grzesik et al. [26]. TiN coatings provide wear coefficients as low as 6×10^{-15}–10×10^{-15} m^3/Nm. For the TiN–MoS_x composite coating, the same could be as low as 0.5×10^{-15} m^3/Nm [25]. Similarly, wear coefficients of around 10×10^{-15} m^3/Nm [27] or even in the range of 20×10^{-15}–80×10^{-15} m^3/Nm [28] have been reported for TiAlN coatings. In the present study, the coatings obtained from pure targets provided wear resistance in the range of 5.6–9.5×10^{-15} m^3/Nm, which is better than the reported values. Though the coatings obtained using alloyed targets provided better coating thickness, higher composite micro-hardness and higher critical load (for sample S11), such coatings yielded poor wear resistance, as has been noted in Table 4. Such a high value of wear coefficient (26×10^{-15} m^3/Nm) could be attributed to the possible removal of overgrowths, as seen in Fig. 2, during the ball-on-disc test.

Machining performance can be evaluated by assessing different machinability criteria, namely, cutting forces, cutting temperature, product quality, tool wear, etc. Tool wear and tool life are the most important machinability criteria having direct industrial relevance. In the present work, the machining performance of the coated inserts has been primarily evaluated using the tool wear criterion. Dry turning has been performed as dry machining is gradually becoming more industrially relevant [29]. Figure 3 shows the growth of average flank wear against machining time whilst dry turning SAE 1020 steel bar of 160-mm diameter at a cutting speed of 250 m/min, feed of 0.2 mm/rev and a depth of cut of 2 mm. Though the break-in wear performance of all the inserts looks very similar, the beneficial effect of using alloyed targets becomes very evident after around 100 s of machining. The average flank wear as well as the rate of growth of flank wear for samples S10 and S11 (obtained using alloyed target) are significantly better than the coated tools obtained using pure targets. The literature suggests that a high coating thickness may not be suitable for machining as the coating may spall due to lack of toughness. Posti and Nieminen [30] noted that the tool life increased in turning up to a maximum coating thickness of 6 μm, and the same Q9 increase was noted with coating thickness around 2–3 μm in the case of interrupted cutting. A similar effect of coating thickness has been reported by Tuffy et al. [31] for TiN deposited using CFUBMS. Thus, one may infer that alloyed targets have provided thicker coatings and that the thickness of the coating has played a significant beneficial role in

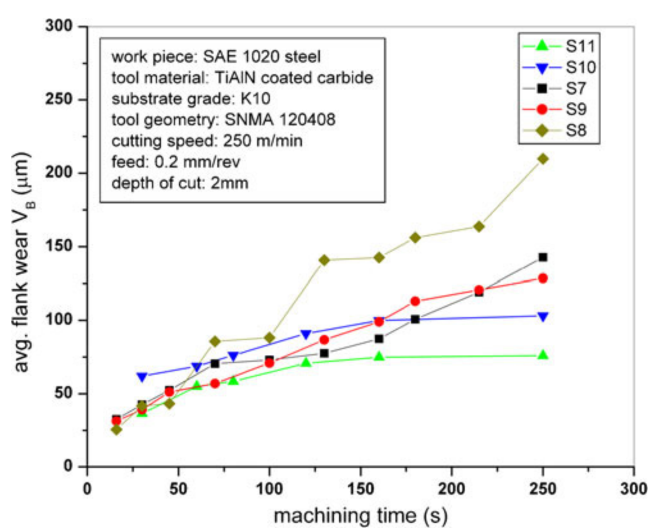

Fig. 3 Growth of average flank wear against machining time whilst dry turning of SAE 1020 steel at a cutting speed of 250 m/min, feed of 0.2 mm/rev and a depth of cut of 2 mm

JrnlID 170_ArtID 4360_Proof# 1 - 03/07/2012

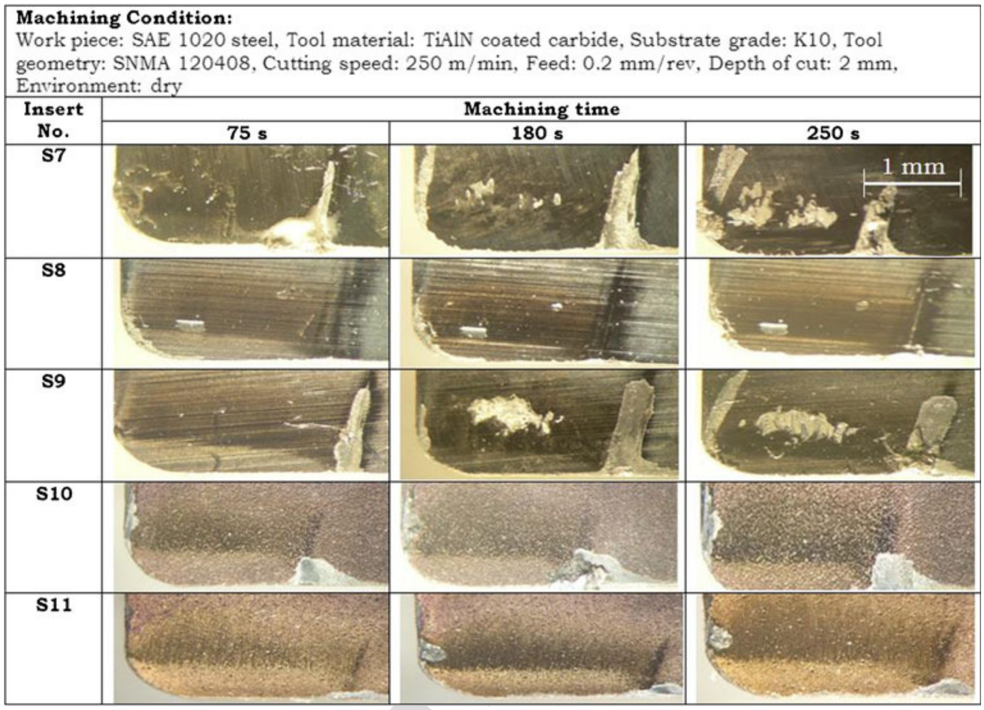

Fig. 4 Nature and extent of crater wear of different inserts after dry turning of SAE 1020 steel at a cutting speed of 250 m/min, feed of 0.2 mm/rev and a depth of cut of 2 mm

improving wear resistance of the coated tool during the dry turning despite opposing views expressed in the literature. Interestingly, the performance of sample S11 is even better than sample S10. This may be attributed to the benefit of a higher target frequency on the coating characteristics, as documented by Kelly and Arnell [32] and Bhaduri et al. [19]. In the present study also, sample S11 provided higher composite micro-hardness and critical load as compared to sample S10, which may have as well contributed to its better machining performance.

The nature and the extent of crater wear and flank wear on different inserts after dry turning of SAE 1020 steel have been revealed in Figs. 4 and 5, respectively. It may be emphasized that the photomicrographs have been taken after cleaning the inserts in acidic solution. Inserts coated using pure targets (S7, S8 and S9) started developing main

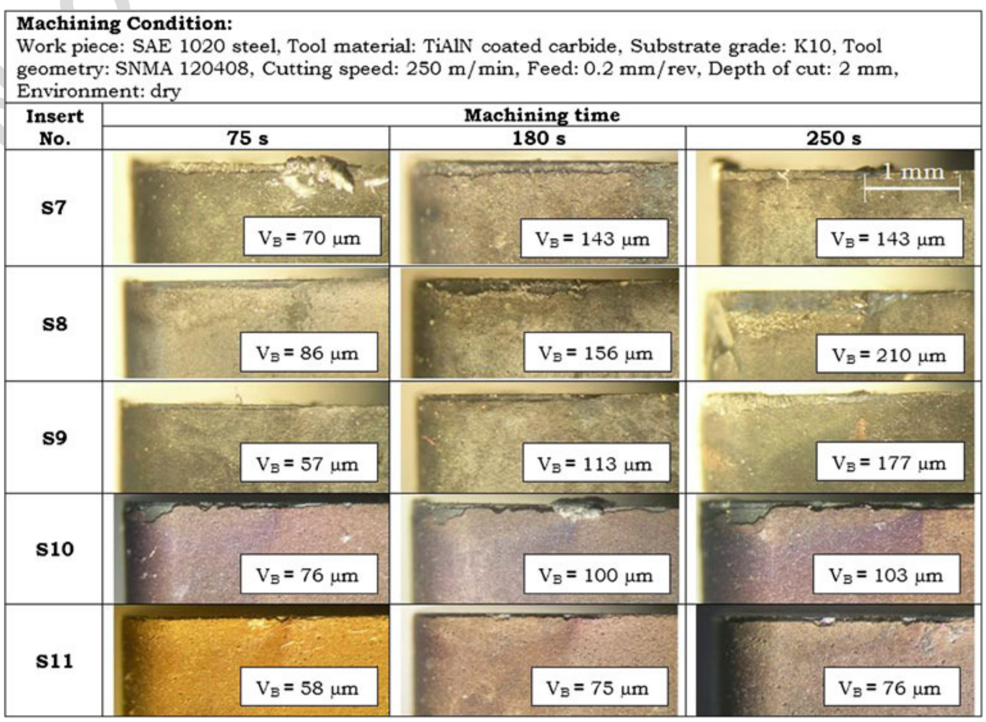

Fig. 5 Nature and extent of flank wear of different inserts after dry turning of SAE 1020 steel at a cutting speed of 250 m/min, feed of 0.2 mm/rev and a depth of cut of 2 mm

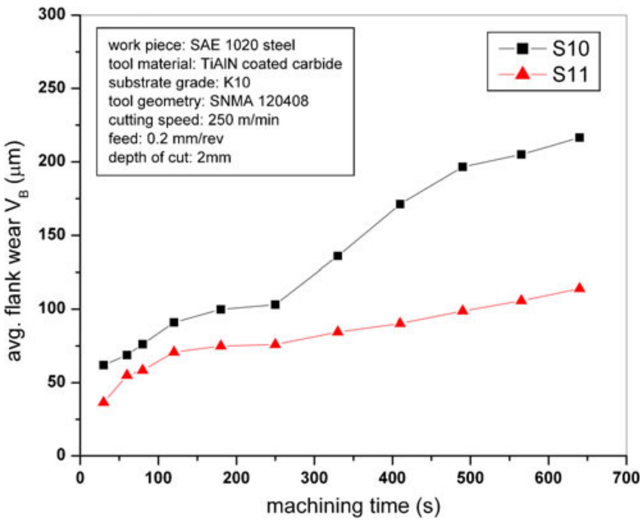

Fig. 6 Growth of average flank wear of inserts S10 and S11 against the machining time whilst dry turning of SAE 1020 steel at a cutting speed of 250 m/min, feed of 0.2 mm/rev and a depth of cut of 2 mm

grooving wear on the rake surface within 75 s of machining. For all the above three inserts, partial removal of coating from the crater surface also started appearing within 180 s. There has also been the appearance of auxiliary grooving wear on the rake surface. Sample S10 (obtained from alloyed target at 200-kHz target frequency) did show removal of the coating at the location of the grooving wear after 75 s of machining, but its extent has been significantly less compared to inserts S7, S8 and S9. S11 (obtained from alloyed target at 300-kHz target frequency) clearly shows suppression of the development of primary grooving wear or removal of the coating even after machining for 250 s, exhibiting once again the benefit of a higher target frequency.

Figure 5 clearly reveals the tendency of material built-up on the cutting edge, particularly for S7 inserts, which could not be removed even by acid etching. Flank wear seems to be uniform, but in excess of 140 μm on inserts coated using pure targets. For example, S8 yielded an average flank wear of 210 μm after 250 s of machining. Insert S10 (obtained from alloyed target at a 200-kHz target frequency), after 250 s of machining, provided 103 μm of average flank wear, but the coating was removed toward the nose of the tool. It seems flank wear has developed more because of coating removal rather than abrasion, indicating poor adhesion between the coating and the substrate. Furthermore, lack of coating toughness could also be the reason for such coating removal from the flank surface, as has been mentioned earlier by Posti and Nieminen [30] and Tuffy et al. [31]. S11, on the other hand, provided a flank wear of only 76 μm after 250 s of machining.

Superior machining performance of samples S10 and S11 is clearly revealed in Figs. 3, 4 and 5 in dry turning. Thus, it was decided to continue dry turning of SAE 1020 steel with only these two inserts up to 640 s; the growth of average flank wear on S10 and S11 inserts has been shown in Fig. 6. The excellent machining performance of S11 is clearly visible in Fig. 6, when it provided average flank wear of only 114 μm after almost 11 min of machining.

No literature could be found to directly compare the present result. Jindal et al. [7] reported the comparative performance of different PVD-coated tools in the machining of SAE 1045 steel, which is also a plain carbon steel but with a nominal carbon percentage of 0.45 %. They obtained tool life in excess of 1 h when the insert was coated with TiAlN coating using a magnetron sputtering process. It may be mentioned that they used the tool life criterion of 0.4 mm of average flank wear. The chosen cutting velocity was 305 m/min, which is 22% more than the present cutting velocity. But the feed and depth of cut were significantly less, by around 25 and 62 %, respectively. The material removal rate (MRR) was only 34 % of the MRR in the present study. Moreover, they employed a coolant during machining. Khrais and Lin [8] investigated the wear mechanism of commercial TiAlN PVD-coated inserts whilst dry machining AISI 4140 steel, which is a low-alloy steel having a carbon percentage of 0.4 % with nickel (0.1 %) and molybdenum (0.2 %) as alloying elements. Dry turning at a cutting velocity of 260 m/min yielded a tool life of around

Table 5 Comparative machining performance

	Time	VB_{max} (mm)	Max. flank wear rate ($\times 10^{-6}$ mm/s)	MRR (mm^3/s)	MRR/wear rate ($\times 10^6$ mm^2)	Carbon equiv. CE	MRR×CE/wear rate ($\times 10^6$ mm^2)
Khrais and Lin: AISI 4140 steel as work material with feed of 0.14 mm/rev and depth of cut of 1 mm							
310 m/min	10 min	0.55	900	723.33	0.79	0.567	0.448
260 m/min	20 min	0.33	200	606.67	2.18		1.236
	25 min	0.61	400	606.67	1.48		0.839
210 m/min	10 min	0.09	100	490	3.15		1.786
	20 min	0.11	92.6	490	5.29		2.999
SAE 1020 steel as work material with cutting velocity of 250 m/min, feed of 0.2 mm/rev and depth of cut of 2 mm							
S11 250 m/min	10 min, 40 s	0.203	0.0003	1,666.67	5.26	0.332	1.746

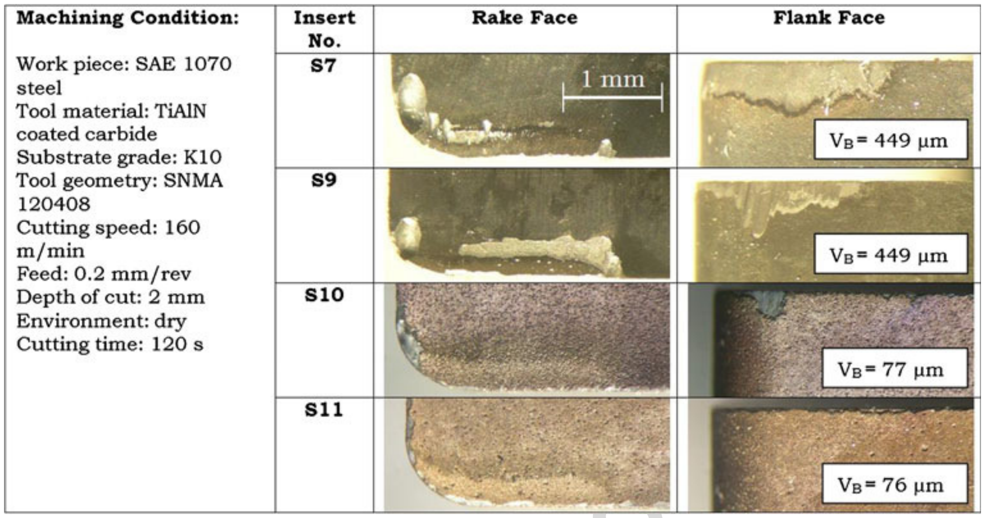

Fig. 7 Nature and extent of crater and flank wear of different inserts after 120 s of dry turning of SAE 1070 steel at a cutting speed of 160 m/min, feed of 0.2 mm/rev and a depth of cut of 2 mm

22 min for a tool life criterion of 0.6 mm of maximum flank wear. They employed a depth of cut of 1 mm (50 % less than the present depth of cut) and a feed of 0.14 mm/rev (30 % less than the present feed).

To enable a more meaningful comparison between the cutting performances of the present coated inserts with the same from the literature, the following strategy has been adopted. In grinding, resistance to wheel wear is evaluated using a grinding ratio, which is the ratio of the material removal rate to the wear rate [33]. Similarly, Table 5 presents the ratio of the material removal rate to the rate of growth of maximum flank wear. For benchmarking, data from Khrais and Lin [8] have been used as they have also undertaken dry turning. The said ratio has been varied between 0.79 and 5.29×10^6 mm^2 for different cutting velocities at different stages of machining, as has been extracted from the work of Khrais and Lin [8]. The same ratio is as much as 5.26×10^6 mm^2 for the present TiAlN-coated insert (S11). This indicates competitive performance of the presently developed inserts with respect to the machining performance available in the literature.

However, one may argue that two work materials are different. Carbon equivalent has been used for a long time in area welding to judge the hardenability and hardness of weldment of plain and low-carbon steels. This approach allows a comparison of the results even if the steels are of different chemical compositions [34]. The concept of carbon equivalent has also been used in machining by Capello [35]. A higher carbon equivalent would indicate the availability of more carbide-forming elements and more tool wear during machining. Thus, the above proposed ratio of the material removal rate to the rate of growth of maximum

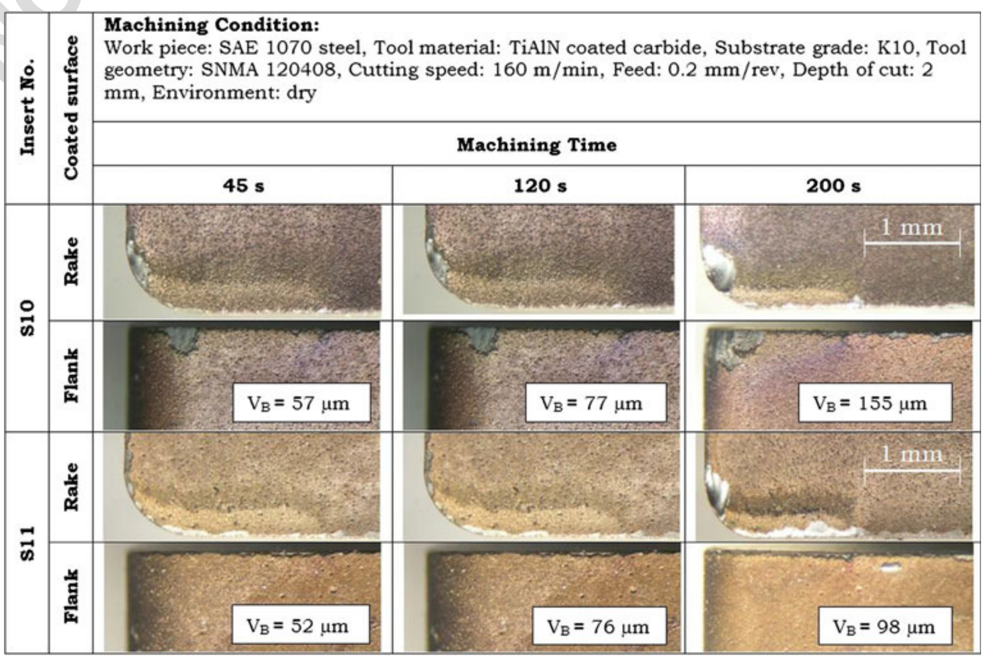

Fig. 8 Nature and extent of crater and flank wear of S10 and S11 after 200 s of dry turning of SAE 1070 steel at a cutting speed of 160 m/min, feed of 0.2 mm/rev and a depth of cut of 2 mm

Q14

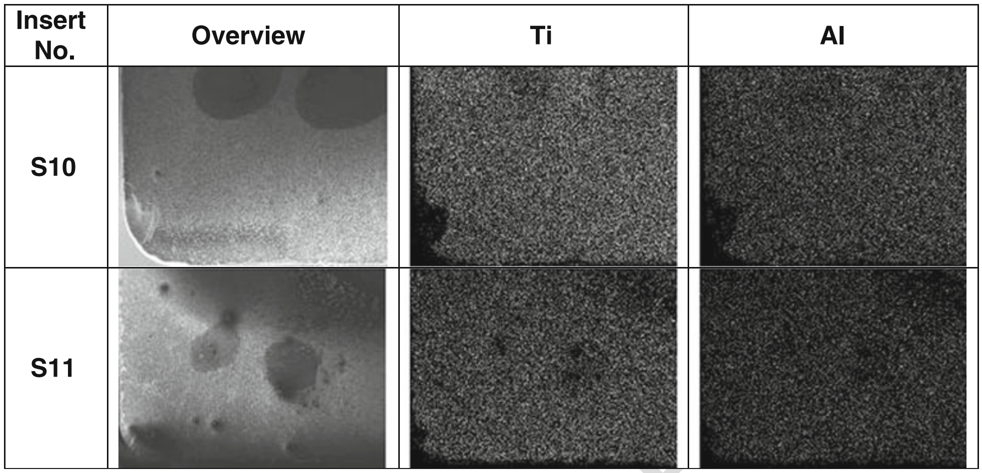

Fig. 9 Elemental area mapping on inserts S10 and S11 after 120 s of dry turning of SAE 1070 steel at a cutting speed of 160 m/min, feed of 0.2 mm/rev and a depth of cut of 2 mm

flank wear is re-modified by multiplying the same by the carbon equivalent. This proposes taking care of the difference in the chemical compositions in the work material. Table 5 indicates the modified ratio which varied between 0.448 and 2.999×10^6 mm^2 for the work undertaken by Khrais and Lin [8]. The same ratio has been found to be 1.746×10^6 mm^2 in the present case. Thus, one may infer that the present cutting tools coated using alloyed targets (particularly sample S11) are very similar in performance to commercially coated inserts despite being deposited in a dual-cathode system.

In the present work, dry turning of SAE 1070 steel was also conducted at a cutting velocity of 160 m/min with a feed and depth of cut of 0.2 mm/rev and 2 mm, respectively. Figure 7 shows the nature and extent of flank and crater wear on selected inserts after 120 s of machining. Overall, inserts coated using alloyed targets are far superior in machining performance. S11 once again establishes its better performance compared to the other inserts. This is also clearly visible in Fig. 8 when machining was continued until 200 s. Figure 9 shows the elemental area mapping on S10 and S11 inserts after 120 s of machining. It is evident that the coating has not been removed from the rake surface of S11 and has only been partially damaged on the rake surface of S10.

4 Conclusion

TiAlN coating could be successfully deposited on uncoated carbide inserts using both pure and alloyed targets via dual-cathode, pulsed DC reactive unbalanced sputtering route. Pure targets provided coating thickness in the range of 2 μm, whereas coating thickness in excess of 12 μm could be obtained from alloyed targets.

The scratch test provided critical load in the range of 50–90 N, though the effect of the type of target was not evident. Wear coefficients as obtained by the ball-on-disc tribological test is acceptably low in the range of $5–9\times10^{-15}$ m^3/Nm for coatings from pure targets. Coatings deposited from alloyed targets yielded poor wear coefficients in the ball-on-disc tribological test.

SAE 1020 steel bar could be efficiently dry turned at 250 m/min for more than 4 min with all the inserts. However, the average flank wear on the coated inserts obtained from alloyed targets was substantially less than that on inserts coated using pure targets. When machining was continued until almost 11 min, one of the inserts only underwent an average flank wear of around 115 μm. Such machining performance is comparable to previously reported ones despite being deposited using dual-cathode deposition systems, unlike four- or six-cathode systems.

Even dry turning of SAE 1070 high-carbon steel at 160 m/min did not yield more than 100 μm of average flank wear on the same insert coated using alloyed targets for a machining time of more than 3 min.

Acknowledgment The authors gratefully acknowledge the funding support received from the Department of Science and Technology, Government of India, under FIST programme (sanction no. SR/FST/ET-II-003/2000 dated 20.5.2002).

References

1. Munz WD (1986) Titanium aluminium nitride films: a new alternative to TiN coatings. J Vac Sci Technol, A 4:2717
2. Lee KH, Park CH, Yoon YS, Lee JJ (2001) Structure and properties of Ti Cr N coatings produced by the ion-plating method. Thin Solid Flims 385:167–173
3. Santana AE, Karimi A, Derflinger VH, Schutze A (2004) Thermal treatment effects on microstructure and mechanical properties of TiAlN thin films. Tribol Let 17(4):689–696
4. McIntyre D, Greene JE, Hakansson G, Sundgren JE, Munz WD (1990) Oxidation of metastable single phase polycrystalline $Ti_{0.5}$ $Al_{0.5}$ N films: kinetics and mechanisms. J Appl Phys 67(3):1542–1553
5. Hsieh JH, Liang C, Yu CH, Wu W (1998) Deposition and characterization of TiAlN and multi-layered TiN/TiAlN coatings using

unbalanced magnetron sputtering. Surf Coat Technol 108–109:132–137

6. Kelly PJ, Abu-Zeid OA, Arnell RD, Tomg J (1996) The deposition of aluminium oxide coatings by reactive unbalanced magnetron sputtering. Surf Coat Technol 86–87:28–32
7. Jindal PC, Santhanam AT, Schleinkofer U, Shuster AF (1999) Performance of PVD TiN, TiCN, and TiAlN coated cemented carbide tools in turning. Int J Refract Met Hard Mater 17:163–170
8. Khrais SK, Lin YJ (2007) Wear mechanisms and tool performance of TiAlN PVD coated inserts during machining of AISI 4140 steel. Wear 262:64–69
9. Musil J, Hruby H (2000) Superhard nanocomposite $Ti_{1-x}Al_xN$ films prepared by magnetron sputtering. Thin Solid Films 365:104–109
10. Zhou T, Nie P, Cai X, Chu PK (2009) Influence of N_2 partial pressure on mechanical properties of (Ti, Al)N films deposited by reactive magnetron sputtering. Vacuum 83:1057–1059
11. He Y, Apachitei I, Zhou J, Walstock T, Duszczyk J (2006) Effect of prior plasma nitriding applied to a hot-work tool steel on the scratch-resistant properties of PACVD TiBN and TiCN coatings. Surf Coat Technol 201:2534–2539
12. Chattopadhyay AK, Chattopadhyay AB (1984) Wear characteristics of ceramic cutting tools in machining steel. Wear 93:347–359
13. Chattopadhyay AK, Chattopadhyay AB (1982) Wear and performance of coated carbide and ceramic tool. Wear 80:239–258
14. Venkatesh VC, Ye CT, Quinto DT, Hoy DEP (1991) Performance studies of uncoated, CVD-coated and PVD-coated carbides in turning and milling. CIRP Ann Manuf Technol 40(1):545–550
15. Gekonde HO, Subramanian SV (2002) Tribology of tool–chip interface and tool wear mechanisms. Surf Coat Technol 149:151–160
16. Konyashin IY (1995) PVD/CVD technology for coating cemented carbides. Surf Coat Technol 71:277–283
17. Alberdi A, Margin M, Diaz B, Sanchez O, Escobar Galindo R (2007) Wear resistance of titanium–aluminium–chromium–nitride nanocomposite thin films. Vacuum 81:1453–1456
18. Q15 Veldhuis SC, Dosbaeva GK, Elfizy A, Fox-Rabinovich GS, Wagg T (2010) Investigations of white layer formation during machining of powder metallurgical Ni-based ME 16 superalloy. J Mater Eng Perform 19(7):1031–1036
19. Bhaduri D, Ghosh A, Gangopadhay S, Paul S (2010) Effect of target frequency, bias voltage and bias frequency on microstructure and mechanical properties of pulsed DC CFUBM sputtered TiN coating. Surf Coat Technol 204:3684–3697
20. Oliveira JC, Manaia A, Cavaleiro A (2008) Hard amorphous Ti–Al–N coatings deposited by sputtering. Thin Solid Films 516:5032–5038
21. Astrand M, Selinder TI, Sjostrand ME (2005) Deposition of $Ti_{1-x}Al_xN$ using bipolar pulsed dual magnetron sputtering. Surf Coat Technol 200:625–629
22. Oliveira JC, Manaia A, Dias JP, Cavaleiro A, Teer D, Taylor S (2006) The structure and hardness of magnetron sputtered Ti–Al–N thin films with low N contents (<42%). Surf Coat Technol 200:6583–6587
23. Shum PW, Li KY, Zhou ZF, Shen YG (2004) Structural and mechanical properties of titanium–aluminium–nitride films deposited by reactive closed-field unbalanced magnetron sputtering. Surf Coat Technol 185:245–253
24. Zywitzki O, Klostermann H, Fietzke F, Modes T (2006) Structure of superhard nanocrystalline (Ti, Al)N layers deposited by reactive pulsed magnetron sputtering. Surf Coat Technol 200:6522–6526
25. Gangopadhyay S, Acharya R, Chattopadhyay AK, Paul S (2009) Composition and structure–property relationship of low friction, wear resistant TiN–MoS_x composite coating deposited by pulsed closed-field unbalanced magnetron sputtering. Surf Coat Technol 203:1565–1572
26. Grzesik W, Zalisz Z, Krol S, Nieslony P (2006) Investigation on friction and wear mechanisms of the PVD–TiAlN coated carbide in dry sliding against steel and cast iron. Wear 261:1191–1200
27. Mo JL, Zhu MH, Lei B, Leng YX, Huang N (2007) Comparison of tribological behaviours of AlCrN and TiAlN coatings—deposited by physical vapour deposition. Wear 263:1423–1429
28. Li X, Li C, Zhang Y, Tang H, Li G, Mo C (2010) Tribological properties of the Ti–Al–N thin films with different components fabricated by double-targeted co-sputtering. Appl Surf Sci 256:4272–4279
29. Klocke F, Eisenblatter G (1997) Dry cutting. CIRP Ann Manuf Technol 46(2):519–526
30. Posti E, Nieminen I (1989) Influence of coating thickness on the life of TiN-coated high speed steel cutting tools. Wear 129:273–283
31. Tuffy K, Byrne G, Dowling D (2004) Determination of the optimum TiN coating thickness on WC inserts for machining carbon steel. J Mater Process Technol 155–156:1861–1866
32. Kelly PJ, Arnell RD (2000) Magnetron sputtering: a review of recent developments and applications. Vacuum 56:159–172
33. Malkin S (1989) Grinding technology—theory and applications of machining with abrasives. Society of Manufacturing Engineers, Michigan
34. Lancaster JF (1999) Metallurgy of welding. Abington Publishing, Cambridge
35. Capello E (2006) Residual stresses in turning: part II. Influence of the machined material. J Mater Process Technol 172:319–326

AUTHOR QUERIES

AUTHOR PLEASE ANSWER ALL QUERIES.

Q1. Please check captured corresponding author if appropriate.
Q2. Occurrences of “dc” were changed to “DC”. Please check.
Q3. Please check value here if appropriately presented.
Q4. Please check presentation of this entry if appropriate.
Q5. Please check changes made to this sentence.
Q6. Figures 2,4,5 & 8 contains small and blurry text. Please provide better quality of image, otherwise, please advise if okay to proceed as is.
Q7. Please check change made here.
Q8. Please check whether this sentence is appropriately presented.
Q9. “tool life increased in turning upto a maximum coating thickness of 6 m and the same was around 2–3 m in case of interrupted cutting” was changed to “tool life increased in turning up to a maximum coating thickness of 6 µm, and the same increase was noted with coating thickness around 2–3 µm in the case of interrupted cutting”. Please check.
Q10. Please check changes made to this sentence.
Q11. Please check merging made here if appropriate.
Q12. Please check changes made here.
Q13. Please check change in sentence presentation made here.
Q14. Figure 9 has discrepancy between pdf and tiff file, we proceed using pdf file since it has vector objects/text.
Q15. Ref. 18 was not cited anywhere in the text. Please provide a citation. Alternatively, delete the item from the list.